Magnetooptical properties and FMR in granular nanocomposites $(\mathbf{Co}_{84}\mathbf{Nb}_{14}\mathbf{Ta}_2)_x(\mathbf{SiO}_2)_{100-x}$

Victoria E. Buravtsova[1], Vladimir S. Guschin[1*], Yuri E. Kalinin[2],
Sergey A. Kirov[1], Eugenia V. Lebedeva[1], Songsak Phonghirun[1],
Alexander V. Sitnikov[2], Nikolay E. Syr'ev[1], Igor' T. Trofimenko[1]

[1] *Physics Faculty,*
Lomonosov Moscow State University,
Leninskie Gory, 119899, Moscow, Russia

[2] *Department of Solid State Physics,*
Voronezh State Technical University,
Moskovsky Prospekt 14, 394026, Voronezh, Russia

Abstract: For nanodimensional magnetically inhomogeneous amorphous granular films of the system $(Co_{84}Nb_{14}Ta_2)_x(SiO_2)_{100-x}$, $30 \leq x \leq 60$ at.% the concentration dependences of the magnetooptical Kerr effect (MOKE) spectra and FMR have been investigated. The observed changes in the MOKE and FMR spectra are associated with transformations of microstructure and topology of the nanocomposites. For the compositions within the percolation region the transversal Kerr effect increases by an order of magnitude.

© Central European Science Journals. All rights reserved.

Keywords: magnetooptic, FMR, granular films
PACS (2000): 78.20.Ls

1 Introduction

From the beginning, nanocrystalline materials of the ferromagnetic-dielectric type have attracted attention of both engineers and researchers. Early experiments demonstrated a number of important transport properties, including the giant magnetoresistance (MR) [1] and the giant Hall effect [2]. Nevertheless, interest was not restricted to the magneto-transport properties of such nanostructures. In some of them linear and non-linear mag-

---

* E-mail: guschin@genphys.phys.msu.ru

netic and magnetooptical (MO) effects have been found in the visible and near IR range [3, 4]. It was also shown that for a wide range of compositions of amorphous granular films containing magnetic nanoclusters (CoNbTa, CoFeZr, CoFeB) imbedded into the silicon oxide matrix [5, 6], the optical and magnetooptical properties differed drastically from the ones of the corresponding bulk materials and exhibited strong dependence on various structural parameters. Generally, electric, magnetic, and optical properties of granular metal-dielectric structures depend on the ferromagnetic phase concentration and experience radical changes when the composition goes beyond the percolation threshold. The most conspicuous magnetic field response of the nanocomposites in percolation region is the emergence of the giant tunnel magnetoresistance (GMR) [4, 7] and a giant magnetooptical effect, the magnetorefractive effect (MRE), which is non-linear in magnetization magnitude [8-11]. In the IR range, the magnetorefractive effects demonstrate a specific frequency dependence and exceed the traditional odd and even MO effects by an order of magnitude and even more. In general, it is clear that the mechanisms both of the GMR and MRE are determined by the spin-dependent scattering and spin-dependent tunneling of polarized electrons between ferromagnetic granules across the dielectric interlayers. Yet there is no complete understanding of the physics of these and other related effects. In particular, there is no satisfactory explanation of the concentration dependence of the electrical resistivity, magnetic and magnetooptical properties and absorption of electromagnetic waves in the SHF range. These problems are of interest not only for the fundamental science but are important for realization of practical tasks, first of all for creation of nanostructural materials which applications are very promising and have already begun: they are used in highly sensitive magneto-resistive sensors and miniature magnetic read/write heads for the high density information-carrying media, selective amplifiers and modulators of the light, thermal radiation receivers, electrochromic displays etc.

Here, we present investigation of structural, magnetic, and magnetooptical properties of nano-dimensional magnetically inhomogeneous materials. The problems discussed below deal with formation of the magnetically ordered state in granular structures composed of ferromagnetic nano-dimensional CoNbTa particles inside the dielectric SiO_2 matrix and with the dependence of the above properties on the concentration and size of magnetic granules. The research makes use of two UHF structure-sensitive spectroscopic methods, the magnetooptical one in the optical range and FMR in the SHF range.

2 Samples. Preparation and structure

Granular amorphous films containing nano-dimensional clusters of the $Co_{84}Nb_{14}Ta_2$ alloy randomly distributed in the insulating amorphous matrix SiO_2 were prepared in argon atmosphere by ion-beam sputtering of compound targets, containing both the ferromagnetic and the dielectric components, on uncooled pyroceram substrates. The choice of a rather complicated composition of the granules $Co_{84}Nb_{14}Ta_2$ was determined by the requirement to stabilize the amorphous structure of the ferromagnetic at room temperatures. Usu-

ally for this purpose, the ferromagnetic cobalt is alloyed with 16–25 % of amorphizators. A characteristic feature of our alloy is the use of metallic amorphizators niobium and tantalum instead of metalloids. Moreover, the amorphous alloy $Co_{84}Nb_{14}Ta_2$ possesses a rather low saturation magnetostriction magnitude ($\lambda_s \approx 0,5 \cdot 10^{-6}$). The choice of the silicon oxide as a material for the matrix was by no means accidental but determined by its thermal stability in a wide temperature range.
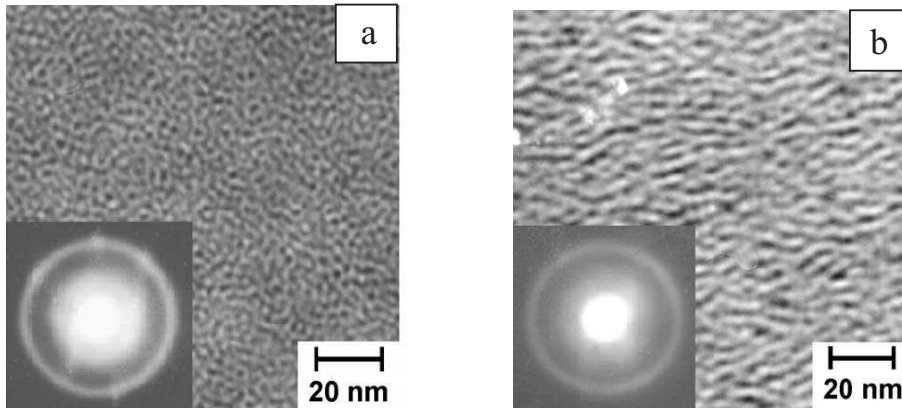

Fig. 1 Photomicrographs and electron diffraction patterns of granular nanocomposites $(Co_{86}Ta_{12}Nb_2)(SiO_n)_{100-}$: a– $(Co_{86}Ta_{12}Nb_2)_{34}(SiO_n)_{66}$; b– $(Co_{86}Ta_{12}Nb_2)_{42}(SiO_n)_{58}$.

During simultaneous sputtering of the metallic alloy and of the dielectric from the compound target, a fragmented structure is formed composed of metallic amorphous granules imbedded inside the dielectric matrix, with a wide and continuous range of the ferromagnetic phase concentrations x from 30 to 60 at.% being obtained. The manufactured film samples were about 2 μm thick. When the concentration of SiO_2 was maximal, the average size of ferromagnetic granules sputtered on a static substrate was 2–4 nm. With decrease of the dielectric fraction the size of ferromagnetic granules increases, and in nanocomposites with large concentrations of the metallic phase ($x = 50$–60 at.%) it becomes 5–7 nm. The structure and morphology of the samples have been investigated by transmission electron microscopy. The electron diffraction pattern of one of the granular nanocomposites $(Co_{84}Nb_{14}Ta_2)_x(SiO_2)_{100-x}$, shown as an example in Fig. 1, demonstrates that the structure is amorphous. Composition of the samples has been checked by the electron probe X-ray spectrum microanalysis.

When the SiO_2 content is high, most of the metallic granules are isolated from each other and behave as superparamagnetic particles. However, some of them are combined in small conglomerates and strings. Analysis of the data on the concentration dependence of magnetoresistivity demonstrates (Fig. 2) that its noticeable growth begins at comparatively small x (around 36 at.%), being connected with tunneling that begins at these concentrations. The maximum of the magnetoresistivity effect is observed around the percolation threshold (46 at.%). At this point, the conductivity mechanism changes from the one based on electron tunneling over the dielectric matrix to the metallic one through the conducting channels which form a fractal structure composed of amorphous granules of $Co_{84}Nb_{14}Ta_2$ contacting with each other. At $x \approx 55$ at.%, the magnetoresistance

vanishes.

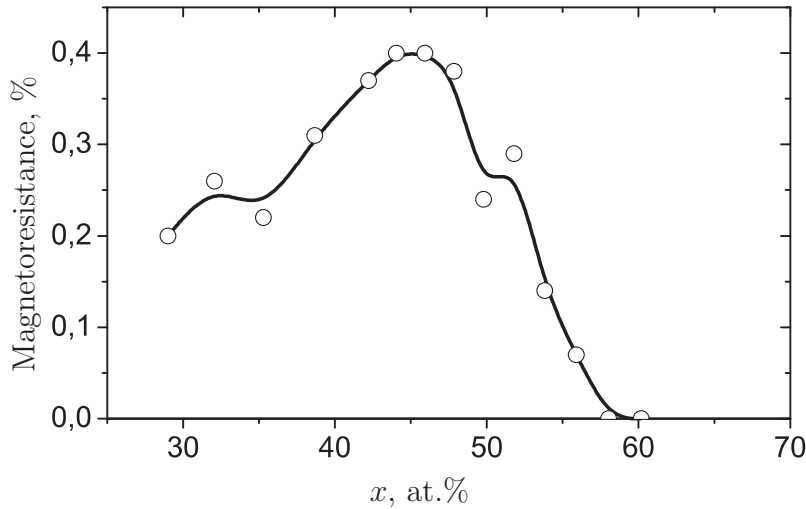**Fig. 2** Concentration dependence of magnetoresistance for a $(Co_{84}Nb_{14}Ta_2)_x(SiO_2)_{100-x}$ granular nanocomposite.

3 Experiment and discussion

3.1 Magnetooptical properties

The magnetooptical properties have been studied by the transversal Kerr effect (TKE). It consists of relative change of the intensity of the linearly polarized light (p-wave) reflected from the sample in the case when magnetization vector is parallel to the surface and at the same time lies perpendicular to the incident light plane (the transversal geometry):

$$\delta = \frac{I_H - I_{H=0}}{I_{H-0}}. \tag{1}$$

Here, I_H and $I_{H=0}$ are intensities of the light reflected by the magnetized and non-magnetized samples, respectively. The measurements of TKE have been performed using a dynamic method developed for measuring MO-effects [12] in which the remagnetization of the sample by the AC magnetic field leads to a modulation of the reflected light intensity, the depth of which determines the magnitude δ of the MO effect. The TKE spectra $\delta(h\nu)$ and the magnetic field dependence curves $\delta(H)$ have been measured in the 0,5–4,0 eV photon energy range for the incidence angle $\varphi = 70°$ in the AC magnetic field of 78 Hz frequency and amplitude up to 1,5 kOe.

The curves of the TKE frequency dependence $\delta(h\nu)$ of amorphous granular nanocomposites $(Co_{84}Nb_{14}Ta_2)_x(SiO_2)_{100-x}$ shown in Fig. 3 substantially differ from both the corresponding spectra of the polycrystalline cobalt [12] and the amorphous alloy $Co_{84}Nb_{14}Ta_2$, characteristic feature of the latter, common to other amorphous Co and Fe-based alloys [13], being the frequency independent TKE in the energy range $h\nu > 2,0$ eV. The most profound changes of $\delta(h\nu)$ have been found in the range $h\nu < 1,5$ eV. Conversely, in the

alloy $Co_{84}Nb_{14}Ta_2$ and in Co the TKE magnitude drops to zero with decrease of the energy of photons ($\delta(h\nu) \approx 0$ at $h\nu = 0{,}7$ eV) in the nanocomposites $\delta(h\nu)$ changes its sign and attains maximum negative values in the $0{,}7 - 1{,}2$ eV interval. In this region the absolute values of TKE of the nanocomposites are 5 times greater than the ones observed in the amorphous alloy $Co_{84}Nb_{14}Ta_2$. One should keep in mind that in the amorphous granular nanocomposites which demonstrate the greatest TKE magnitudes, the magnetic phase content is virtually two times less than that in the amorphous alloy $Co_{84}Nb_{14}Ta_2$. It should also be mentioned that in this region the TKE $x-$dependence is non-monotonous. The maximum changes of TKE occur in the samples with magnetic phase concentrations within the region 45–50 at.%, which corresponds to the percolation threshold. A similar behavior of the TKE concentration dependence has been observed in the system of granular films composed of silicon oxide with nanoparticles of CoNbTa [14].
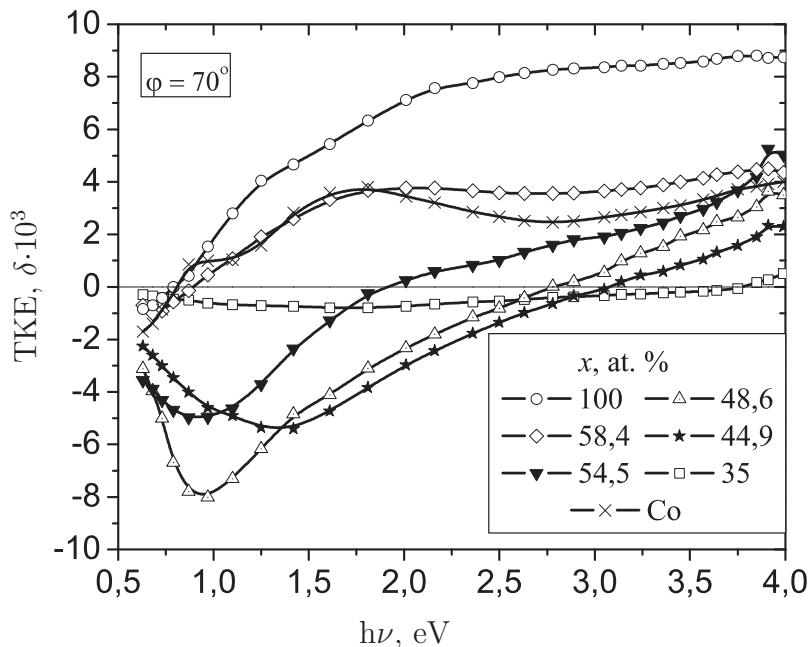

Fig. 3 Despersion of TKE in the nanocomposites $(Co_{84}Nb_{14}Ta_2)_x(SiO_2)_{100-x}$.

In nanocomposites with larger concentrations of the ferromagnetic phase the spectra change their shape in such a way that the region where TKE is positive increases. At the same time for the nanocomposite with $x = 58{,}4$ at.%, the TKE zero point position coincides with the corresponding zeros both for pure Co and the amorphous alloy $Co_{84}Nb_{14}Ta_2$. In the visible light range, a frequency independent part of the TKE spectrum begins to develop in samples with magnetic phase concentration above 54 at.%.

The curves of the TKE magnetic field dependence (Fig. 4) measured at $h\nu = 1{,}42$ eV demonstrate that nanocomposites with various content of the ferromagnetic phase exhibit different magnetization mechanisms. When concentration of the ferromagnetic granules is small, the TKE magnitude increases linearly with the magnetic field up to $H = 1{,}5$ kOe. In the vicinity of x_{per} and in the region $x > x_{per}$, the saturation of δ is achieved. More clearly, the character of the TKE magnetic field dependence can be seen in Fig. 6 where each of the curves $\delta(H)$ is normalized to the magnitude of the effect in the field 1,5 kOe.
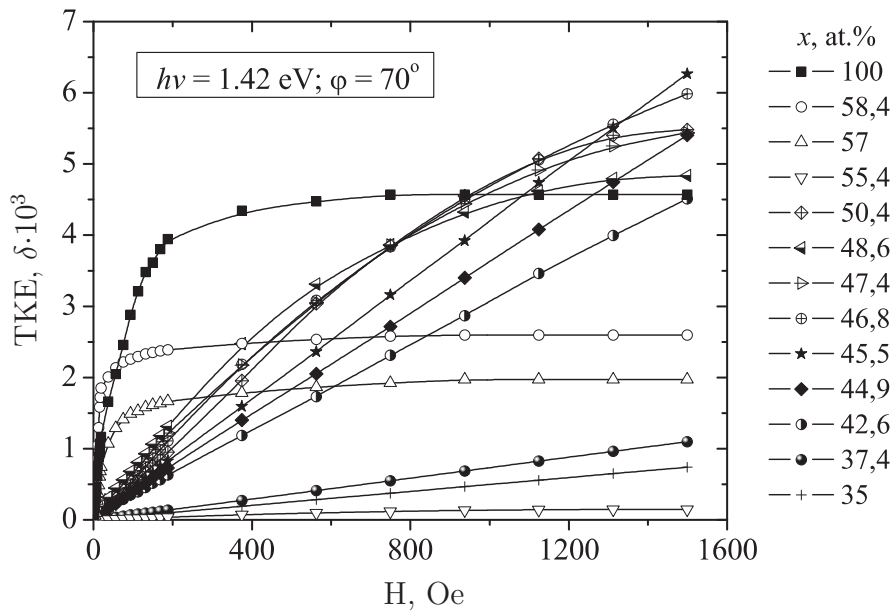
Fig. 4 Magnetic field dependences of TKE in nanocomposites $(Co_{84}Nb_{14}Ta_2)_x(SiO_2)_{100-x}$.

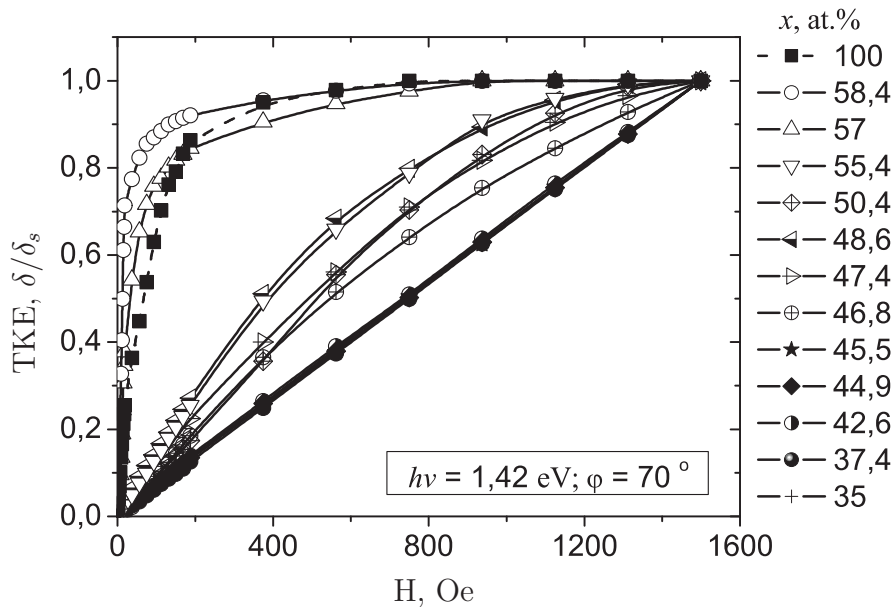**Fig. 5** Normalized values of field dependences of TKE in nanocomposites $(Co_{84}Nb_{14}Ta_2)_x(SiO_2)_{100-x}$.

Three concentration regions can be singled out, each corresponding to particular magnetization mechanisms. The samples of the first group with metallic phase concentration x < 45 at% belong to the pre-percolation group. Their $\delta(H)$ curves exhibit the behavior typical for superparamagnetics (linear dependence of $\delta(H)$ up to 1,5 kOe). The samples of the second group with concentrations corresponding to the percolation region ($45 < x$ < 55 at.%) demonstrate another type of dependence, while the samples with the maximum concentration practically being magnetized to saturation in the fields $\sim$ 1,5 kOe. The nanocomposites with $x > 55$ at.%, i.e. beyond percolation threshold, exhibit magnetization of the ferromagnetic type. For them the saturation typically takes place in the

fields less than 0,2 kOe. These results are in a good agreement with the data of structural investigations and rf spectroscopy, confirming that in the pre-percolation region most of the granules are well isolated from each other, do not interact and demonstrate superparamagnetic behavior. When x increases, the size of the granules grows, the separating dielectric interlayers naturally becoming thinner. The magnetic momentum of the nanocomposite increases due to the growth of the magnetic phase volume.

In summary, the MO investigations demonstrate that in magnetically ordered nanocomposites composed of the amorphous metal-amorphous dielectric the MO effect in the near IR region becomes substantially larger, almost by an order of magnitude for the compositions close to percolation. There is no doubt that the growth of the MO effects is connected both with transformations of microstructure and topology of the granular alloys which produce changes in the character of electron conductivity, magnetoresistance etc., and with the changes of the optical and MO parameters of nanocomposites [6, 11].

3.2   Ferromagnetic resonance

The FMR spectra have been recorded with an EPR spectrometer at the frequency $\omega/2\pi = 9450$ MHz using the standard modulation method. The resonance field H_r and resonance linewidth ΔH of the homogeneous precession mode was measured at various orientations of the DC magnetic field $\boldsymbol{H}$ relative the film normal $\boldsymbol{n}$. For all orientations of $\boldsymbol{H}$, the rf magnetic field $\boldsymbol{h}$ remained perpendicular to $\boldsymbol{n}$. In all cases, the variation of the film plane orientation relative to the DC magnetic field was achieved by rotation of the sample. The measurements were performed at room temperature.

The observed orientation dependence of the FMR magnetic fields for the homogeneous precession mode was found to obey closely the conventional formula [14, 15] (Fig. 10b).

$$\left(\frac{\omega}{\gamma}\right)^2 = (H_r \cos\alpha - H_{eff}\cos\theta)^2 + H_r \sin\alpha \ (H_r \sin\alpha + H_{eff}\sin\theta) \tag{2}$$

with the following equation determining the equilibrium state

$$2H_r \sin(\theta - \alpha) = H_{eff}\sin 2\theta, \tag{3}$$

where α and θ are the angles between the film normal and directions of magnetic field $\boldsymbol{H}$ and magnetization $\boldsymbol{M}$ correspondingly (inset in Fig. 9) and γ is the gyromagnetic ratio. The effective field takes into account the demagnetizing fields and the field of magnetic anisotropy: $\boldsymbol{H}_{eff} = \boldsymbol{H}_{dem} + \boldsymbol{H}_a$. Fig. 6 demonstrates the dependence of H_r on x for the angles $\alpha = 0$ and $\alpha = 90°$. For $x < 38$ at.% the resonance fields for both directions are close to each other. Further increase of x leads to the growing divergence between the $H_r(\alpha = 0)$ and $H_r(\alpha = 90°)$ curves.

Using the equations (2), (3), and the obtained experimental data $H_r(\alpha)$, the magnitudes of $H_{eff}(x)$ (Fig. 7) and γ have been calculated. For the samples with $x = 38$–55 at.%, the magnitude of γ within our experimental accuracy remains constant and close to 2,8. The figure also shows the magnetization magnitude $4\pi M_s$ for some of the
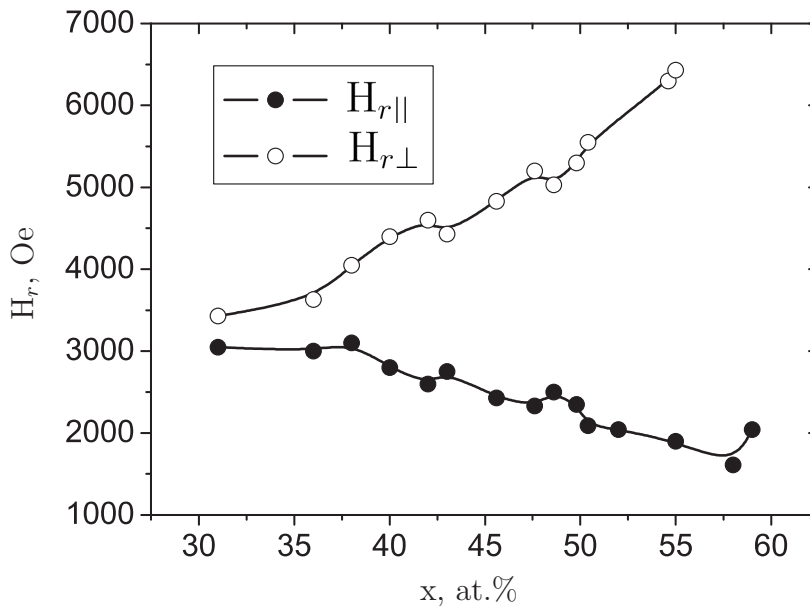
Fig. 6 Parallel ($H_{r||}$) and perpendicular ($H_{r\perp}$) resonance fields as functions of x.

samples measured with a vibrating sample magnetometer. The results demonstrate that H_{eff} is governed mainly by demagnetization fields for $30 < x < 50$ at.%. For $x > 50$ at.% the perpendicular anisotropy appears. Both $H_{eff}(x)$ and $4\pi M_s(x)$ are non-linear in x. This result coincides with the data reported in [14] and [15] for the samples containing granules of Co in the non-magnetic matrix of CuO or Ag and, in the authors' opinion [14], explained by contributions to the magnetization from the para- and superparamagnetic particles that are present in the samples for all x. Their quantity is determined by the average size of the granules.

The linewidth ΔH was found to be most sensitive to structural changes in the material of the samples. Fig. 8 shows the curves $\Delta H(x)$ for the in-plane ($\alpha = 90$) and normal magnetization ($\alpha = 0°$). Here it is possible to differentiate three regions with different behavior of $\Delta H(x)$. The boundaries of the regions demonstrate a good correlation with the MO data.

For nanostructures with x within 31–45 at.%, ΔH exhibits a very weak dependence both on x (Fig. 8) and on the orientation of the DC field $\boldsymbol{H}$ (Fig. 10a, curve 1). Magnetic measurements show that magnetization curves of these samples coincide for all the magnetization directions, and in the fields up to 6000 Oe the magnetization magnitude practically linearly depends on H. Photomicrographs demonstrate that for these concentrations most of the microgranules are of spherical shape and are surrounded by the non-magnetic matrix. These data, as well as the magnetooptical data testify that in the concentration interval up to 45 at.% the nanocomposites behave similar to superparamagnetics.

For x within 45–54 at.%, the behavior of the ΔH concentration dependence exhibits a drastic change. The absorption signal grows by more than one order of magnitude. The magnitude of $\Delta H_{||}(x)$ decreases smoothly with a slightly increasing slope. $\Delta H_{\perp}(x)$ for x
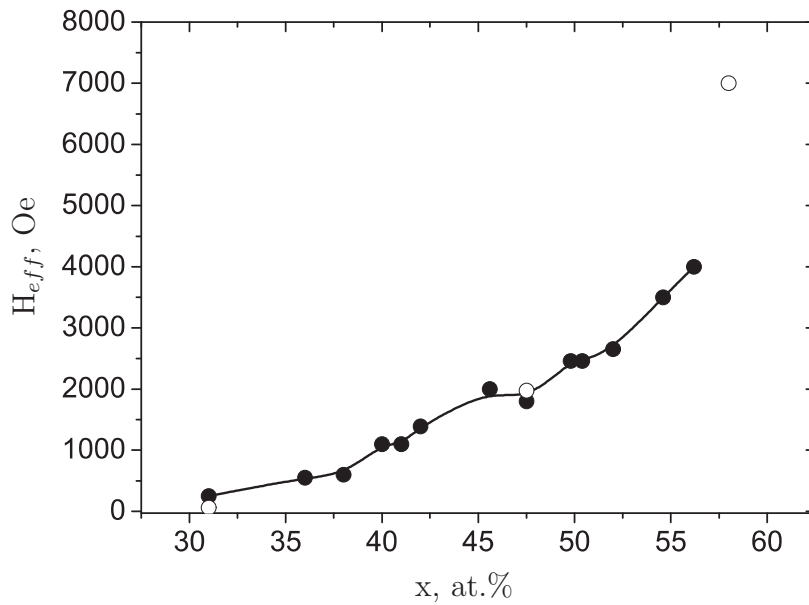
Fig. 7 The x at.% content dependence of H_{eff} and $4\pi M_s$. $\bullet - H_{eff}$, $\circ - 4\pi M_s$.
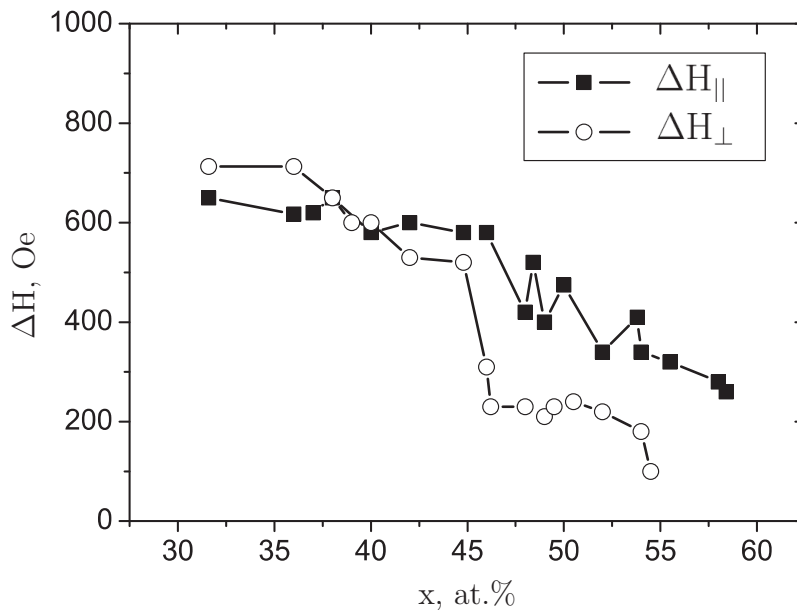

Fig. 8 Parallel and perpendicular linewidth versus magnetic phase concentration x.

= 45 at.% demonstrates an abrupt and almost twofold decrease and then remains nearly constant. Photomicrographs distinctly show that at these concentrations a change both in the shape and topology of the granules occurs. They are of an elongated form and combined in chains.

For concentrations $x < 48$ at.% the FMR spectra contain only one line for all orientations of $\boldsymbol{H}$ (Fig. 9a,b). For $x > 48$ at.% and when the direction of $\boldsymbol{H}$ is close to the film normal, additional resonances appear in the fields below the resonance field of the main homogeneous precession mode (Fig. 9c). The maximum magnitude of ΔH was observed at intermediate orientations of the magnetic field (Fig. 10a, curve 2).

To explain the results we have used a simple model [16-18] assuming that ΔH of
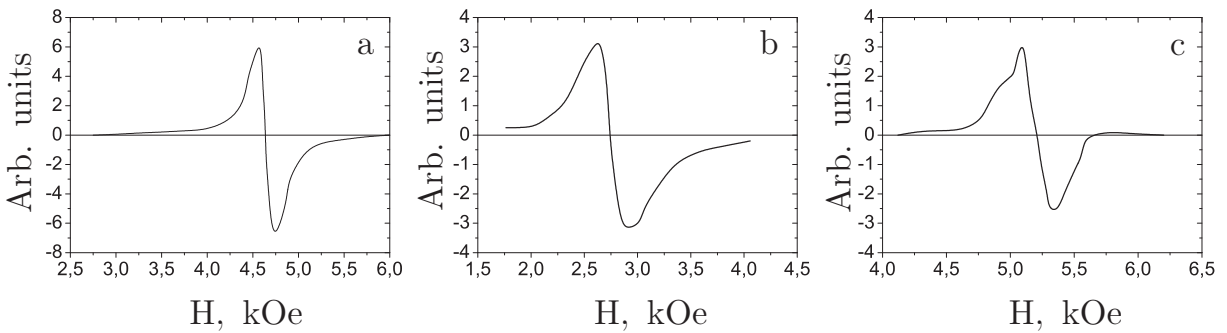
Fig. 9 FMR spectrum of $(Co_{84}Nb_{14}Ta_2)_{46}(SiO_2)_{54}$ (**a** $- \alpha = 0$; **b** $- \alpha = 90°$) and of $(Co_{84}Nb_{14}Ta_2)_{52}(SiO_2)_{48}$ (**c** $- \alpha = 10°$).

homogeneous mode is determined by superposition of resonance lines of separate non-interacting granules having different magnitudes of H_r. The granules were represented as randomly oriented ellipsoids with the long axis lying in the film plane. The computations based on this model actually yield $\Delta H_{||} > \Delta H_{\perp}$. Yet to obtain a satisfactory agreement between the calculated and experimental values of ΔH, it is necessary to assume that the spread in granule orientations is rather small (this assumption does not contradict the data of microphotographs). However it is not clear why the abrupt changes in the shape and orientations of the granules proceeding at the percolation threshold should manifest themselves primarily in the magnitude of $\Delta H_{\perp}$.

In the region of large magnetic phase concentrations above 54 at.% in the samples with the smallest losses the dependence of $\Delta H_{||}$ on x does not experience modifications: with increase of x the $\Delta H_{||}$ magnitude continuously drops approaching the magnitude of $\Delta H_{||}$ of the bulk amorphous alloy (180–200 Oe) $\Delta H_{\perp}$ is also decreasing. For such x the spectra become rather complicate in character. As before, with α varying from 90° to 30° the linewidth ΔH of the main resonance is increasing. The absorption curve becomes notably deformed. In the fields below H_r a wide pedestal appears, and in the strong fields emerges a wide absorption peak. The further increase of α leads to an abrupt diminution of ΔH (Fig. 9a, curve 3) and the resonance line restores its usual shape, although in the fields both below and above H_r up to six small resonance peaks appear.

It should be noted that the samples with the same x corresponding to large metallic phase content exhibit a considerable spread both of H_r (1000–2500 Oe) and ΔH (80–600 Oe) thus demonstrating that in the samples with large magnetic phase concentrations there can be formed regions with different cluster size resulting in various demagnetizing fields.

4 Conclusions

Complex investigations of static and hf properties of granulated composite films $(Co_{84}Nb_{14}Ta_2)_x(SiO_2)_{100-x}$ as functions of ferromagnetic phase concentration x ($30 < x < 60$ at.%) have been carried out. The measurements included resistivity, magnetoresistance, magnetization, transversal Kerr effect (TKE in the 0,5–4,0 eV band), angular
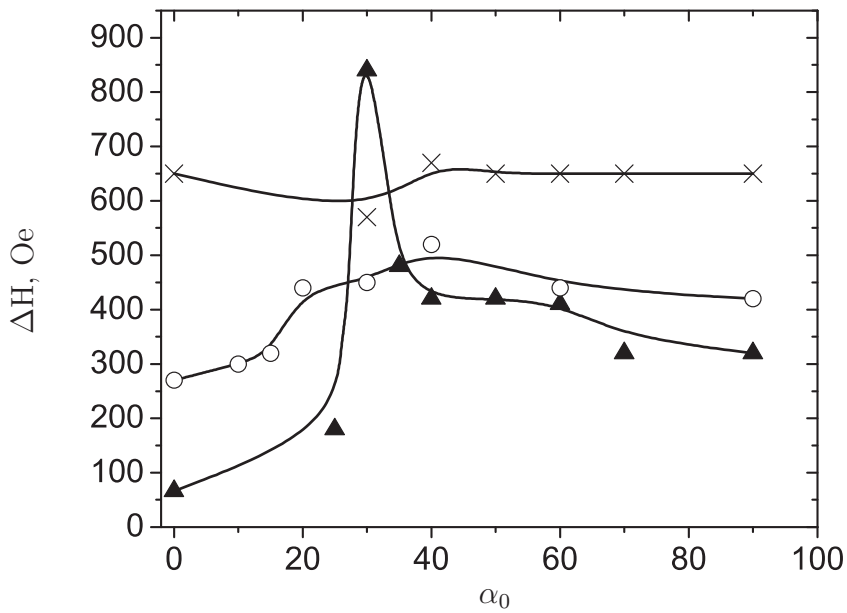
a)
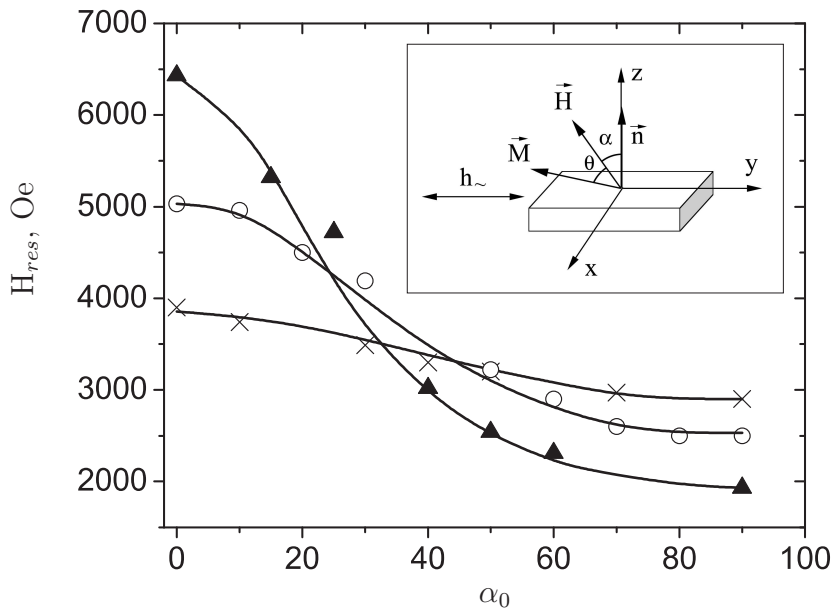
b)

Fig. 10 a) Angular dependence of the FMR linewidth for the samples with x, at.%: 1–38; 2–48,6; 3–55. b) Angular dependence of the resonance fields for the samples with x, at.%: 1–38; 2–48,6; 3–55 with H_{eff}, Oe: 1–450, 2–1860, 3–3300. Solid lines — theory. Points — experiment.

dependencies of ferromagnetic resonance spectra (f = 9400 MHs). Combining the data on structural, magnetooptical, magneto-transport properties and FMR we may conclude that they are in agreement with each other and confirm the existing concepts of formation of nanostructural ferromagnetics with large magnetoresistance.

The system obviously shows certain percolation properties with threshold value x= 46–48 at.%. In this region essential changes of most of their characteristics appear. In

particular, the most profound nonlinear changes of TKE have been revealed near the threshold. In the near IR band the absolute value of TKE increases by an order of magnitude as compared with that of amorphous alloys of the same chemical composition. A sharp decrease in the uniform precession mode linewidth was observed in FMR spectra for the magnetic field normal to the film surface.

The observed changes in the MOKE and FMR spectra are connected with transformations of microstructure and topology of magnetic nanocomposites.

We thank very much prof. N.S. Perov for his valuable magnetic measurements and useful discussions.

References

[1] S. Mitani, H. Fujimori, K. Takanashi, K. Yakusiji, J.-G. Ha, S. Takahashi, S. Maekawa, S. Ohnuma, N. Kobayashi, T. Masumoto, M. Ohnuma and K. Hono: "Tunnel-MR and spin electronics in metall-nonmetall granular systems", *Journal of Magnetism and Magnetic Materials*, Vol. 198-199, (1999), pp. 179–184.

[2] A. Pakhomov, X. Yan and Y. Xu: "Observation of giant Hall effect in granular magnetic films", *Journal of Applied Physics,* Vol. 79, (1996).

[3] O.A. Aktsipetrov, E.A. Gan'shina, V.S. Guschin, T.V. Misuryaev and T.V. Murzina: "Magneto-induced second harmonic generation and magneto-optical Kerr effect in Co-Cu granular films", *Jornal of Magnetism and Magnetic Materials*, Vol. 196-197, (1999), pp. 80–82.

[4] M. Gester, A. Schlapka, R.A. Pickford, S.M. Thompson, J.P. Camplin, J.K. Eve and E.M. McCash: "Contactless measurement of giant magnetoresistance in CoAg granular films using infrared transmission spectroscopy", *Journal of Applied Physics*, Vol. 85, (1999), pp. 5045–5047.

[5] V.E. Buravtsova, E.A. Gan'shina, V.S. Guschin, Yu.E. Kalinin, S. Phonghirun, A.V. Sitnikov, O.V. Stogney and N.E. Syr'ev: "Gigantskoe magnitosoprotivlenie i magnitoopticheskie svoystva granulirovannih nanokompozitov metall-dielektric", *Izvestiya Rossiiskoi Akademii Nauk Seriya Fizicheskaya*, Vol. 67(7), (2003), pp. 918–920.

[6] E.A. Gan'shina, A.B. Granovsky, V.S. Guschin, Yu.E. Kalinin, P.N. Scherbak, A.V. Sitnikov, M.V. Vashuk, A.N. Vinogradov, Chong-Oh Kim and Cheol Gi Kim: "Evolutsiya opticheskih i magnitoopticheskih svoystv nanokompozitov amorfniy metall-dielektric", *Zhurnal Eksperimental'noy i Teoreticheskoy Fiziki*, Vol. 4, (2004).

[7] N. Kobayashi, S. Ohnuma, T. Masumoto and H. Fujimori: "(Fe-Co)-(Mg-fluoride) insulating nanogranular system with enhanced tunnel-type giant magnetoresistance", *Journal of Applied Physics*, Vol. 90, (2001), pp. 4159–4162

[8] I.V. Bykov, E.A. Gan'shina, A.B. Granovsky and V.S. Guschin: "Magnitorefraktivny effekt v granulirovannih plyonkah s tunelnim magnitosoprotivleniem", *Physics of Solid State*, Vol. 42, (2000), pp. 487–491.

[9] D. Bozec, V.G. Kravets, J.A.D. Matthew, S.M. Thompson and A.F. Kravets: "Infrared reflectance and magnetorefractive effects in metal-insulator CoFe-Al$_2$O$_3$ granular films", *Journal of Applied Physics*, Vol. 91(10), (2002), pp. 8759–8762.

[10] A.B. Granovsky, V.S. Guschin, I.V. Bykov, A.A. Kozlov, N. Kobayashi, S. Ohnuma, T. Masumoto and M. Inoue: "Gigantsky magnitorefraktivny effekt v magnitnih

granulirovannih splavah CoFe –MgF", *Physics of Solid State*, Vol. 45(5), (2003), pp. 876–878.

[11] A.B. Granovsky, I.V. Bykov, E.A. Gan'shina, V.S. Guschin, M. Inoue, Yu.E. Kalinin, A.A. Kozlov and A.N. Yurasov: "Magnitorefraktivny effekt v magnitnih nanokompozitah", *Zhurnal Eksperimental'noy i Teoreticheskoy Fiziki*, Vol. 123, (2003) pp. 1256–1266.

[12] G.S. Krinchik and V.S. Guschin: "Issledovanie mezhzonnih perehodov v ferromagnitnih metallah i splavah magnitoopticheskim metodom", *Zhurnal Eksperimental'noy i Teoreticheskoy Fiziki*, Vol. 56, (1969), pp. 1833–1842.

[13] L. Valenchik, E.A. Gan'shina, V.S. Guschin, D.M. Dzhuraev and G.S. Krinchik: "Opticheskie i magnitoopticheskie svoystva amorfnih splavov na osnove zheleza", *Fizika Metetallov Metalloved.*, Vol. 67, (1980), pp. 1108–1116.

[14] A.V. Kimel', R.V. Pisarev, A.A. Rzhevski, Yu.E. Kalinin, A.V. Sitnikov, O.V. Stogne, F. Bentivegna and Th. Rasing : "Magnetooptical Study of Granular Silicon Oxide Films with Embedded CoNbTa Ferromagnetic Particles", *Physics of Solid State*, Vol. 45, (2003), pp. 283–286

[15] G.V. Skrotsky and L.V. Kurbatov: *Fenomenologicheskaya teoriya ferromagnitnogo resonansa", Ferromagnitny Resonanc*, Fizmatgiz., Moscow, 1961.

[16] A. Butera, J.N. Zhou and J.A. Barnard: "Ferromagnetic resonance in as-deposited and annealed Fe-SiO$_2$ heterogeneous thin films", *Physical Review B*, Vol. 60, (1999).

[17] A. Granovsky, N. Perov, O. Fillipov, A. Rakhmanov, J. Clerc and P. Bares: "Mixtures of ferromagnetic and nonmagnetic beads as a model of granular alloys: magnetic properties and impedance", *J. Materials Science Forum*, Vol. 373-376, (2001).

[18] E.A. Gan'shina, V.S. Guschin, S.A. Kirov, N.S. Perov, N.E. Syr'ev and F. Brouers: "Magnetic, magnetooptical properties and FMR in multilayer films (Ni$_{81}$Fe$_{19}$)10Å/Ag", *Journal of Magnetism and Magnetic Materials*, Vol. 165, (1997), pp. 346–348.

[19] E. Shlömann: "Spin-wave analysis of ferromagnetic resonance in polycrystalline ferrites", *Journal of Physical Chemistry of Solids*, Vol. 6(2/3), (1958).

[20] J. Dubowik: "Shape anisotropy of magnetic heterostructures", *Physical Review B*, Vol. 54(2), (1996).

[21] U. Netzelman: "Ferromagnetic resonance of particulate magnetic recording tapes", *Journal of Applied Physics,* Vol. 68(4), (1990), pp. 1800–1806.